

1 Possible influence of atmospheric circulations on winter hazy
2 pollution in Beijing-Tianjin-Hebei region, northern China

3
4 Ziyin Zhang^{1*}, Xiaoling Zhang¹, Daoyi Gong², Seong-Joong Kim³, Rui Mao²,
5 Xiujuan Zhao¹

6 ¹*Environmental Meteorology Forecast Center of Beijing-Tianjin-Hebei, Chinese
7 Meteorological Administration, Beijing 100089, China*

8 ²*State Key Laboratory of Earth Surface Processes and Resource Ecology, Beijing
9 Normal University, Beijing 100875, China*

10 ³*Korea Polar Research Institute, Incheon 406-840, Korea*

11
12 **Abstract:**

13 Using the daily records derived from the synoptic weather stations and the
14 NCEP/NCAR and ERA-Interim reanalysis data, the variability of the winter hazy
15 pollutions (indicated by the mean visibility and number of hazy days) in Beijing-
16 Tianjin-Hebei (BTH) region during the period 1981 to 2015 and its relationship to the
17 atmospheric circulations in middle-high latitude were analyzed in this study. The winter
18 hazy pollution in BTH had distinct inter-annual and inter-decadal variabilities without
19 a significant long-term trend. According to the spatial distribution of correlation
20 coefficients, six atmospheric circulation indices (I_1 to I_6) were defined from the key
21 areas in sea level pressure (SLP), zonal and meridional winds at 850 hPa (U850, V850),
22 geopotential height field at 500 hPa (H500), zonal wind at 200 hPa (U200), and air
23 temperature at 200 hPa (T200), respectively. All of the six indices have significant and
24 stable correlations with the winter visibility and number of hazy days in BTH. In the
25 raw (unfiltered) correlations, the correlation coefficients between the six indices and
26 the winter visibility (number of hazy days) varied from 0.57 (0.47) to 0.76 (0.6) with
27 an average of 0.65 (0.54); in the high-frequency (<10 yr) correlations, the coefficients
28 varied from 0.62 (0.58) to 0.8 (0.69) with an average of 0.69 (0.64). The six circulation
29 indices together can explain 77.7% (78.7%) and 61.7% (69.1%) variances of the winter
30 visibility and number of hazy days in the year-to-year (inter-annual) variability,
31 respectively. The increase of I_c (a comprehensive index derived from the six individual

* Correspondence to: Ziyin Zhang, Environmental Meteorology Forecast Center of Beijing-Tianjin-Hebei, Chinese Meteorological Administration, Beijing 100089, China.
E-mail: zzy_ahgeo@163.com

32 circulation indices) can cause a shallowing of the East Asian trough at the middle
33 troposphere and a weakening of the Siberian high pressure field at sea level, and then
34 accompanied by a reduction (increase) of horizontal advection and vertical convection
35 (relative humidity) in the lowest troposphere and a reduced boundary layer height in
36 BTH and its neighboring areas, which are favorable for the formation of hazy pollutions
37 in BTH winter, and vice versa. The high level of the prediction statistics and the
38 reasonable mechanism suggested that the winter hazy pollutions in BTH can be
39 forecasted or estimated credibly based on the optimized atmospheric circulation indices.
40 However, we also noted that the statistic estimation models would be largely influenced
41 by the artificial control of a pollutant discharge. Thus it is helpful for government
42 decision-making departments to take actions in advance in dealing with probably severe
43 hazy pollutions in BTH indicated by the atmospheric circulation conditions.

44 **Key word:** hazy pollution, visibility, atmospheric circulation, Beijing-Tianjin-Hebei,

45

46 **1 Introduction**

47 Beijing-Tianjin-Hebei (BTH) region is located in northern China, with approximately
48 110 million residents and 216,000 km² in size. As the rapid progress of urbanization
49 and industrial development over the past three decades, the BTH region has become
50 one of China's most economically developed regions and the third economic engine in
51 China. Recently, the Chinese government has been promoting the integration of the
52 three neighboring regions to optimize the industrial layout and improve the allocation
53 of resources. Undoubtedly, the BTH region is becoming more and more important in
54 China or even the world economy in the future. However, the rapid economic growth
55 and urbanization have increased the level of air pollution in recent decades ([Streets et al., 2007](#);
56 [Chan and Yao, 2008](#); [Wang et al., 2009](#); [Wang et al., 2010](#); [Gao et al., 2011](#)).
57 Most of eastern China has frequently suffered from severe haze or smog days in recent
58 years, especially in the BTH region. For example, the continuously hazy pollutions in
59 January 2013 greatly threatened human health and traffic safety ([Kang et al., 2013](#);
60 [Wang et al., 2013](#)). Roughly speaking, the hazy pollution can be attributed to two
61 aspects: pollutant emissions to the lower atmosphere from fossil fuel combustion or
62 construction and favorable meteorological conditions. Meteorological conditions are
63 controlling the occurrence of hazy pollution ([Wu, 2012](#); [Zhang et al., 2013](#)).
64 Specifically, weather conditions play an essential role in the daily fluctuation of air
65 pollutant concentrations ([Zhang et al., 2015](#)).

66 At present, many studies have focused on the physical and chemical properties of
67 pollutants in Beijing and other cities (Feng et al., 2006; Yu et al., 2011; Xu et al., 2013;
68 Zhao et al., 2013). And also studies demonstrated the influence of weather conditions
69 or synoptic situations upon air pollutions (Zhao et al., 2009; Zhang et al., 2015). They
70 elucidated clearly the formation and chemical composition of air pollutants and the
71 dominant meteorological factors on hazy days or during heavy pollution in Beijing and
72 its neighboring areas. On the other hand, some studies demonstrated that the hazy
73 pollution occurring in the BTH region could be strongly affected by the local
74 atmospheric circulations including sea–land and mountain–valley breeze circulations
75 and the planetary boundary layer height (Lo et al., 2006; Liu et al., 2009; Chen et al.,
76 2009; Miao et al., 2015). Recently, Wang et al. (2015) suggested that the reduction of
77 autumn Arctic sea ice leads to anomalous atmospheric circulation changes which favor
78 less cyclone activity and more stable atmosphere and leading to more hazy days in
79 eastern China. Moreover, Wang et al. (2013) showed that east China suffered from
80 severe hazy pollutions in January 2013 may be due to a sudden stratospheric warming
81 over the mid-high latitude of Northern Hemisphere, which lead to an anomalous steady
82 atmosphere dominated in northern China. Thus, it is interesting to examine whether the
83 winter hazy pollution in BTH has been influenced by other known or unknown
84 atmospheric circulations or teleconnections in the mid-high latitude of the Northern
85 Hemisphere and whether there are some potential circulations that can be used for the
86 forecast or evaluation of the winter hazy pollution in BTH. To date, it is not clear about
87 these questions, and a few studies have been performed to explore these issues.

88 Owing to a lack of long-term instrumental records for air pollutant concentration,
89 the understanding of the evolution of air pollution and their relations to atmospheric
90 circulations is limited. In this paper, we intend to use the atmospheric visibility and the
91 number of hazy days derived from the synoptic meteorological stations to denote the
92 evolution of hazy pollution in the BTH region since 1980s. Many studies demonstrated
93 that, in the absence of certain weather conditions (e.g., rain, fog, dust and snowstorm),
94 the visibility is an excellent indicator of air quality because its degradation results from
95 light scattering and absorption by atmospheric particles and gases that can originate
96 from natural or anthropogenic sources (Baumer et al., 2008; Chang et al., 2009;
97 Sabetghadam et al., 2012; Baddock et al., 2014), although visibility was influenced
98 comprehensively by airborne pollutants and meteorological parameters such as relative
99 humidity, wind speed, temperature, pressure and solar radiation (Wen and Yeh, 2010;
100 Deng et al., 2014; Zhang et al., 2015) .

101 The main purpose of this study is to examine the possible relations between the
 102 atmospheric circulations and the winter hazy pollution (the mean visibility and mean
 103 number of hazy days) over the BTH region and investigate the possible physical
 104 mechanism, which could be useful for a prediction of the winter hazy pollution and
 105 could provide a scientific support to the government to take effective measures in
 106 advance to reduce or control the pollutant emission in case of an anomalous circulations
 107 leading to a serious hazy pollution in the region. This paper is organized as follows.
 108 Section 2 describes the data and method used. Section 3 shows major results and
 109 discussions. Conclusion is summarized in section 4.

110 **2 Data and methods**

111 **2.1 Research area and station data**

112 The atmospheric visibility recorded at the 19 synoptic meteorological stations
 113 located in the research area from 1 January 1980 to 28 February 2015 were used (Figure
 114 1). The visibility by human observers is recorded by four times (02:00, 08:00, 14:00
 115 and 20:00, Beijing local time) or three times (08:00, 14:00 and 20:00, Beijing local time)
 116 per day. A good continuous monitoring operation was maintained throughout the entire
 117 period, with the missing data rates for the 19 stations varying from a minimum of 1.7%
 118 to a maximum of 2.1%, with a mean 1.9%. On the other hand, the distribution of the
 119 stations is relatively uniform, indicating that the mean visibility or hazy days is a good
 120 representative for the whole BTH region.

121 In the present study, the days with visibility ≤ 5 km and relative humidity $< 90\%$
 122 at 14:00PM (local time) were defined as hazy days, except the special weather
 123 phenomena occurred at this moment including rain, fog, dust and snow (Schichtel et al.,
 124 2010; Wu et al., 2014;). The mean number of hazy days (\overline{NHD}) of each winter in the
 125 BTH region can be calculated by:

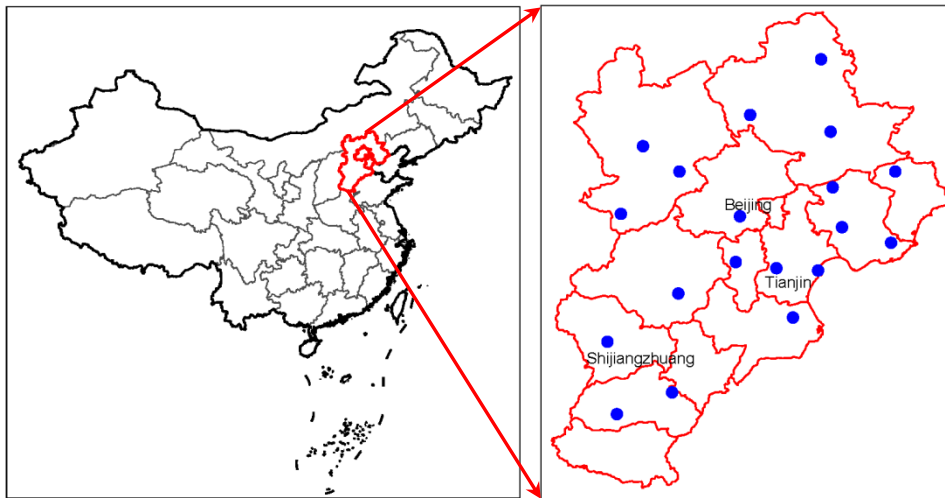
$$126 \quad \overline{NHD} = \frac{1}{n} \sum_{i=1}^n N_i \quad (1)$$

127 where n is the number of stations (here $n=19$), N denotes the number of hazy days
 128 in a station in each winter (December, January and February). The mean visibility (\overline{Vis})
 129 of each winter in the BTH region can be calculated by:

$$130 \quad \overline{Vis} = \frac{1}{n} \sum_{i=1}^n \left(\frac{1}{m} \sum_{j=1}^m V_{ij} \right) \quad (2)$$

131 where n is the number of stations (here $n=19$), m is the number of valid days in

132 winter. It should be noted that the winter in 1981 consists of December 1980, January
133 and February 1981, and so on.



134

135 Figure 1 Research area and locations of the 19 synoptic meteorological stations

136

136 2.2 Reanalysis data

137

137 The global NCEP/NCAR reanalysis data of the monthly sea level pressure (SLP),
138 zonal and meridional winds at 850 hPa (U850, V850), geopotential height field at 500
139 hPa (H500), zonal wind at 200 hPa (U200) and air temperature at 200, 150, 100 and 70
140 hPa (T200, T150, T100, T70) with a $2.5^{\circ} \times 2.5^{\circ}$ spatial resolution from January 1980 to
141 February 2015 were used (Kalnay et al., 1996). Moreover, in order to obtain a higher
142 spatial resolution in the BTH region, the ERA-Interim reanalysis data of the monthly
143 relative humidity (RH), vertical speed (W), zonal (U) and meridional (V) winds from
144 1000 to 500 hPa (16 pressure levels in total) and the boundary layer height (BLH) with
145 a $0.125^{\circ} \times 0.125^{\circ}$ spatial resolution confined to the area $33-45^{\circ}\text{N}$ and $110-122^{\circ}\text{E}$ were
146 also used (Dee et al., 2011).

147

148 2.3 Analysis method

149

149 For the statistical and atmospheric circulation analyses carried out in the study, the
150 common statistical methods such as the composite analyses and the least square
151 regression and the Pearson correlation analyses with a two-tailed Student's t-test were
152 applied in this research. A principal component analysis (PCA) was also used to extract
153 the principal mode of multiple time series. Moreover, in order to reduce the possible
154 effects of low-frequency variation or long-term trends and to examine whether or not
155 the correspondence between the two time series on inter-annual time-scale is stable, the
156 high-frequency ($< 10\text{yr}$) correlation of the high-pass filtered time series was also tested
157 for time series analyses (Gong and Luterbacher, 2008; Zhang et al., 2010).

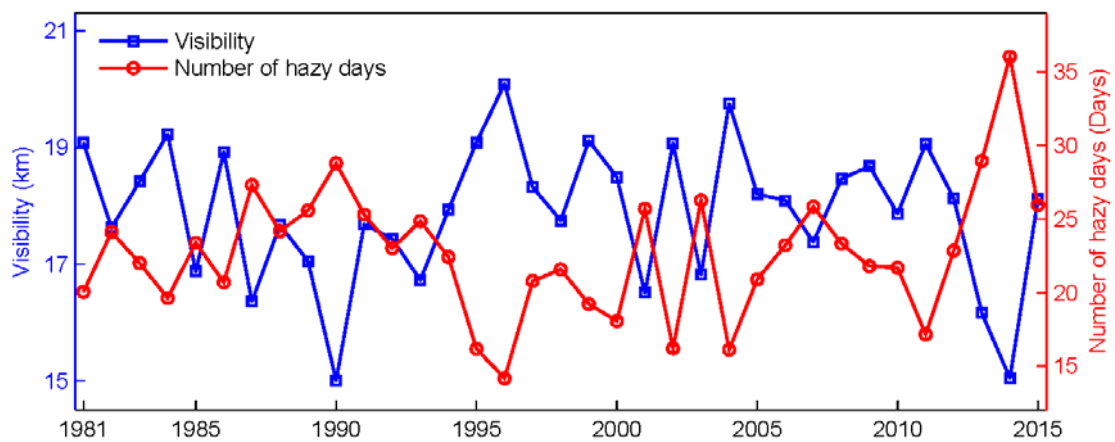
158

159 3 Results and discussions

160 3.1 Evolution of the winter visibility and hazy days in the BTH region

161 The regional mean visibility and number of hazy days in winter in BTH were
162 presented in Figure 2. As expected, the visibility was negatively correlated to the
163 number of hazy days with the raw and high-frequency (< 10yr) correlation coefficients
164 between them of -0.91 and -0.93, respectively. Both of them are significant at the 0.01
165 level ($p < 0.01$ for short). More hazy days generally denote lower mean visibility in
166 winter due to the light scattering and absorption effects of air pollutants (Baumer et al.,
167 2008; Sabetghadam et al., 2012). There are intense inter-annual fluctuations in both the
168 visibility and the number of hazy days over the entire period of 1981 to 2015. The
169 decadal fluctuations can be also distinguished for both the visibility and the number of
170 hazy days throughout the entire period. A significant reducing trend of visibility
171 ($p < 0.05$) and increasing trend of number of hazy days ($p < 0.01$) dominated in the 1980s.
172 And then, the visibility experienced an increasing trend in 1990s and a decreasing trend
173 since 2001, and the hazy days showed an anti-phase changes, but none of them are
174 statistically significant with exception of the number of hazy days trend in 1990s
175 ($p < 0.05$). The mean visibility maximum in 1990s reached to 18.3 km (larger than the
176 mean values of 17.9 km over the entire period); and the minimum number of hazy days
177 in 1990s reached to 20.6 days (less than the mean values of 22.7 days over the entire
178 period). However, the long-term trends of them are not statistically significant, although
179 a weak reducing and increasing trends can be founded in the curves of winter visibility
180 and number of hazy days, respectively.

181



182

183 Figure 2 Curves of the winter mean visibility and number of hazy days in BTH

184

185 **3.2 Relationship between hazy pollution and atmospheric circulations**

186 We first examined the correlation coefficients between the visibility and number of
 187 hazy days and the most common atmospheric teleconnection or oscillation indices over
 188 the mid-high latitude of Northern hemisphere (see Table 1), which could affect the
 189 winter climate variability over China, such as the Arctic Oscillation (AO), the Northern
 190 Atlantic Oscillation (NAO), the Pacific/North American pattern (PNA), the Eurasian
 191 pattern (EU), the Western Pacific pattern (WP) and the Siberian High (SBH) (Wallace
 192 and Gutzler, 1981; Zhang et al., 2009; Gong and Ho, 2012). It can be seen that both of
 193 the raw ($r1$) and high-frequency ($r2$) correlations show that the visibility and number
 194 of hazy days are correlated weakly with the winter AO, NAO and PNA. However, the
 195 visibility is highly positively correlated with EU, WP and SBH; and the number of hazy
 196 days is highly negatively correlated with EU, WP and SBH, most of them are significant
 197 at the 0.01 or 0.05 level.

198

199

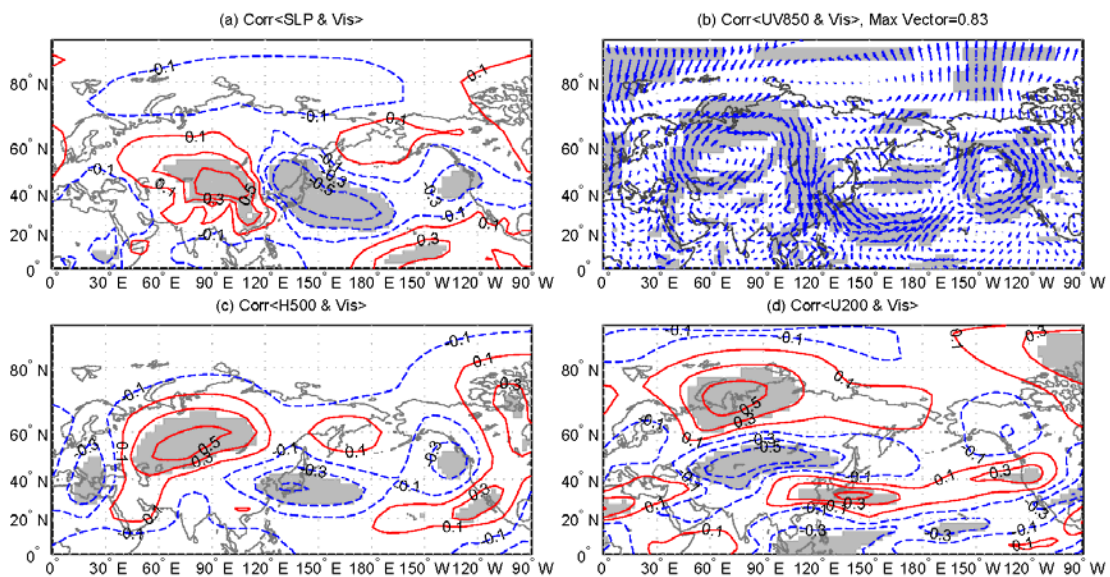
Table 1 Correlation coefficients of visibility and hazy days and circulation indices

		AO	NAO	PNA	EU	WP	SBH
Visibility	$r1$	-0.11	0.00	0.16	0.61**	0.40*	0.39*
	$r2$	0.05	0.22	0.16	0.71**	0.37*	0.36*
Number of hazy days	$r1$	0.13	0.13	-0.10	-0.51**	-0.47**	-0.32
	$r2$	-0.01	-0.11	-0.10	-0.70**	-0.56**	-0.37*

200 ** Significant at the 0.01 level, * Significant at the 0.05 level. The $r1$ and $r2$ terms indicate the
 201 raw correlation and high-frequency (< 10yr) correlation, respectively.

202 Furthermore, the general characteristics of spatial distribution of the correlation
 203 coefficients between visibility and number of hazy days in BTH and the major
 204 meteorological fields from surface to tropopause in Northern Hemisphere including
 205 SLP, U850, V850, H500, U200, T200, T150 and T70 were also examined (Figure 3 and
 206 4). Owing to a generally anti-pattern for the number of hazy days, thus only the
 207 correlation maps with visibility were analyzed for simplicity. In SLP (Figure 3a), a
 208 positive correlation center dominated most of East Asian continent, while a negative
 209 correlation center dominated the area from northeast Asia to northwest Pacific,
 210 respectively. This spatial pattern may reflect the effects of land-sea thermal contrast on
 211 the lower troposphere condition over BTH region. The pressure increasing in East
 212 Asian continent and decreasing in area from northeast Asia to northwest Pacific suggest
 213 that they favor the visibility increase in the BTH region in winter, and vice versa. In
 214 UV850 (Figure 3b), an anomalously anti-cyclonic and northerly pattern are

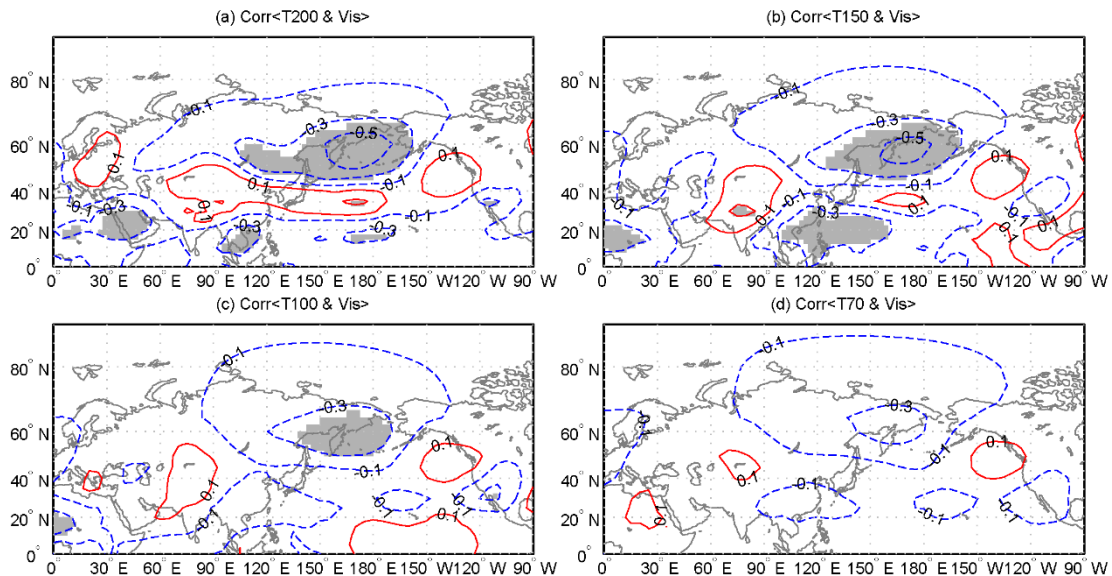
215 predominant most of Siberia and eastern China. This suggests that an anomalous
 216 northerly advection from Siberian to eastern China improve the winter visibility in the
 217 BTH region. In H500 (Figure 3c), there exist a “-+” wave train pattern along the
 218 Eurasia-west Pacific in the mid-high latitude, extending from the central-eastern
 219 Europe through Siberia to north China-Korean peninsula-Japan-northwest Pacific
 220 Ocean, similar to the EU pattern (Wallace and Gutzler, 1981). This pattern implies that
 221 a deepening of East Asian trough and a weakening of blocking will favor the winter
 222 visibility increase in the BTH region. In U200 (Figure 3d), there also exist a wave train
 223 pattern from northwest Russia through Siberia to northwest Pacific Ocean. This pattern
 224 may imply that the south (north) of East Asian Jet stream strengthened (weakened)
 225 coincided with the anomalous ascending (sinking) motions occurred in the south (north)
 226 of the Jet stream entrance at the upper troposphere, which will lead to a strengthening
 227 northerly appeared in the lower troposphere. Hence it is not conducive to the
 228 accumulation of pollutants over BTH region in the winter.
 229



230
 231 Figure 3, Spatial distribution of correlation coefficients between visibility and SLP (a), UV850
 232 (b), H500 (c) and U200 (d) (Area significant at the 0.05 level are shaded; either U850 or V850
 233 significant at the 0.05 level are shaded in b)
 234

235 Besides the lower troposphere, previous studies suggested that the anomalous
 236 stratospheric warming over the Northern Hemisphere led to the severe hazy pollutions
 237 in east China in January 2013 (Wang et al., 2013). Here, the spatial distribution of the
 238 correlation coefficients between visibility and the temperature from the upper
 239 troposphere to lower stratosphere at 200 hPa (T200), 150 hPa (T150), 100 hPa (T100)

240 and 70 hPa (T70) were checked. Negative correlations are found from eastern Siberia
 241 to the northern North Pacific including Alaska in T200, T150, T100 and T70,
 242 respectively (Figure 4), with the biggest correlation in T200 (Figure 4a). The
 243 significantly negative correlation suggest that the warming at 200 hPa over eastern
 244 Siberia to the northern North Pacific would indicate a decreasing of winter visibility,
 245 namely a worsening of hazy pollutions in the BTH region.
 246



247
 248 Figure 4 Spatial distribution of correlation coefficients between visibility and T200 (a), T150 (b),
 249 T100 (c) and T70 (d) (Area significant at the 0.05 level are shaded)
 250

251 Based on the above analyses, we wonder whether the meteorological variables in
 252 the significant correlation areas can be used to predict or evaluate the variability of the
 253 winter visibility and hazy pollutions in the BTH region. Thus, the six indices for
 254 atmospheric circulations or teleconnections were defined based on the key regions
 255 shown in the previous correlation maps as listed in Table 2. We computed the raw and
 256 high-frequency correlation coefficients of the winter visibility and number of hazy days
 257 in BTH and the six atmospheric circulation indices. All of the six indices (I_1 to I_6) show
 258 highly positive or negative correlations with the winter visibility and number of hazy
 259 days, with significance at the 0.01 level (Table3). Moreover, we note that most of the
 260 high-frequency correlations are larger than the raw correlations except the correlations
 261 between visibility and I_1 . This suggests that the links between the air quality in BTH
 262 and the circulations indices are very stable from year to year. The significantly positive
 263 or negative correlations should be a reflection of the physical response mechanisms
 264 between them, which will be discussed in the latter section.

265

266

Table 2 List of the definition for the six circulation indices

Index	Variable	Expression
I ₁	SLP	SLP (38~50N, 84~108E) – SLP (36~52N, 126~150E; 24~40N, 150~184E)
I ₂	U _{850hPa}	U ₈₅₀ (55~75N, 40~110E) – U ₈₅₀ (40~50N, 45~75E)
I ₃	V _{850hPa}	V ₈₅₀ (32~64N, 104~120E)
I ₄	H _{500hPa}	H ₅₀₀ (46~64N, 50~92E) – H ₅₀₀ (28~44N, 16~28E; 28~42N, 120~156E)
I ₅	U _{200hPa}	U ₂₀₀ (42~52N, 60~110E) – U ₂₀₀ (64~76N, 50~96E; 28~36N, 120~152E)
I ₆	T _{200hPa}	T ₂₀₀ (46~66N, 146~196E)

267

268

269

Table 3 Correlation coefficients of visibility and number of hazy days and circulation indices

		I ₁	I ₂	I ₃	I ₄	I ₅	I ₆
Visibility	r1	0.73**	0.57**	-0.76**	0.62**	-0.59**	-0.61**
	r2	0.70**	0.68**	-0.80**	0.72**	-0.62**	-0.62**
Number of hazy days	r1	-0.60**	-0.47**	0.60**	-0.47**	0.52**	0.60**
	r2	-0.61**	-0.65**	0.69**	-0.67**	0.58**	0.64**

270

Same as Table 1

271

272 3.3 Predictions for visibility and number of hazy days based on the circulation 273 indices

274 In order to assess the prediction capability of the six circulation indices for the
275 winter hazy pollutions in BTH, the winter mean visibility and number of hazy days
276 were estimated by applying a multivariate regression method with the least square
277 estimate. The estimated curves by the fitting and the cross-validation with a leave-one-
278 out method were displayed in Figure 5. Intuitively, both of the fitting curves and the
279 cross-validation curves are fairly consistent with the observed winter mean visibility
280 and number of hazy days over the last three decades. The raw and high-frequency
281 correlation coefficients between the observed and the fitting visibility (number of hazy
282 days) are 0.88 (0.78) and 0.86 (0.77), respectively. All of them are significantly at 0.01
283 level. The six circulation indices together can explain 77.7% (78.7%) and 61.7%
284 (69.1%) variances of the winter visibility and number of hazy days over the BTH region
285 in the year to year (inter-annual) variability, respectively. A good fitting does not mean
286 that there must be stable relationships between the dependent variable and explanatory
287 variables. Thus we emphasized testing the stability of the statistic models by means of

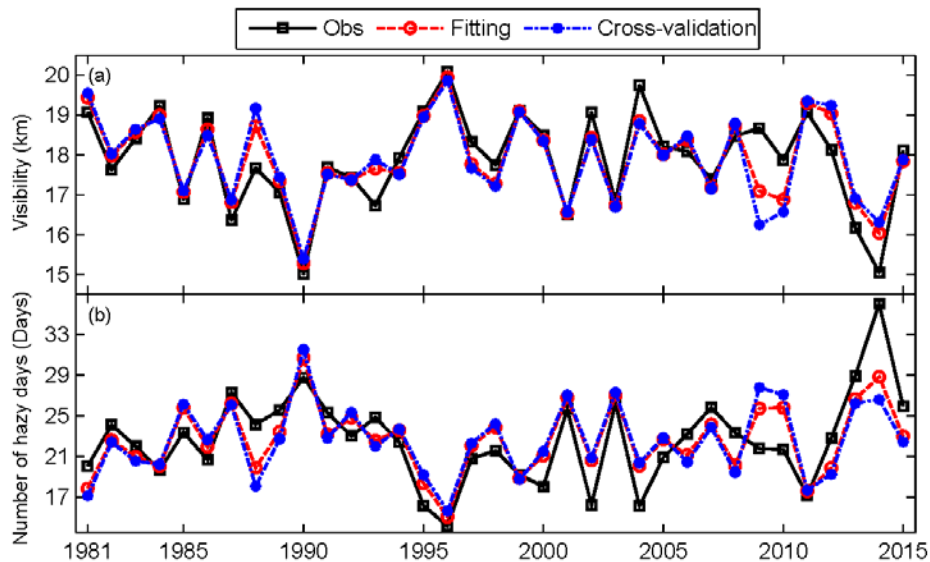
288 the Leave-N-out cross-validations. The statistics for the cross-validation estimations
289 were listed in Table 4, including the explained variance (r^2), the standard error (SE),
290 and reduction of error (RE). Previous studies suggested that RE is an extremely rigorous
291 verification statistic because it has no lower bound, $RE > 0$ indicating the skillful
292 estimation, $RE > 0.2$ indicating the reliable estimation and $RE = 1.0$ indicating a perfect
293 estimation (Fritts, 1976; Gong and Luterbacher, 2008; Zhang et al., 2010).

294 The statistics for both the visibility and number of hazy days are generally stable
295 (no sharply increase or decrease) when N increased from 1 to 11 (more than 30% sample
296 removed in regression models), although the r^2 and RE (SE) slightly decreased
297 (increased) with the increasing of N. For the visibility, the r^2 varied from 52.5% to 62.7%
298 with an average of 57.6%, the SE varied from 0.74 to 0.84 with an average of 0.79, the
299 RE varied from 0.49 to 0.61 with an average of 0.55. For the number of hazy days, the
300 r^2 varied from 31.1% to 41.5% with an average of 35.2%, the SE varied from 3.37 to
301 3.66 with an average of 3.54, the RE varied from 0.23 to 0.38 with an average of 0.30.
302 The mildly changes of these statistics suggest that the statistic models between the given
303 atmospheric circulations and the hazy pollution indicators are stably even in the case of
304 parts of sample missed. On the other hand, we noted the statistics for the visibility
305 estimations are generally better than that for the number of hazy days estimations in all
306 tests. However, the minimum values of r^2 and RE for the number of hazy days
307 estimations are still lager than 30% and 0.2, respectively. Based on these statistics, it
308 can be concluded that the predictions for the winter visibility and number of hazy days
309 in the BTH region based on the circulation indices are overall reliable during the entire
310 period, especially for the mean visibility. That is to say, the winter hazy pollutions in
311 BTH can be evaluated or estimated well by the optimized atmospheric circulations.

312 The relatively larger errors for the estimated values referred to the observed
313 visibility and number of hazy days have been found since the winter in 2009 (Figure 5).
314 We re-computed all the statistics for the period 1981 to 2008, the results displayed that
315 all the values of r^2 and RE (SE) for visibility and number of hazy days predictions
316 increased (decreased) much more than the entire period (Table 4), suggesting that the
317 statistic estimation models are much more stable and reliable before 2009. Why did the
318 prediction efficiency of the statistic estimation models decrease in the last few years?
319 It can be distinguished that the estimations for the winter mean visibility are distinctly
320 lower (higher) than the observed in the winters of 2009 and 2010 (2014), and vice versa
321 for the number of hazy days. We speculated that these phenomena can be attributed to
322 the fluctuations of pollutant emissions in part because the pollutant emissions over

323 northern China around 2008 were controlled strictly by the Chinese government
 324 associated with the 2008 Olympic Games in Beijing (An et al., 2007; Zhang et al., 2010;
 325 Gao et al., 2011). The decrease of pollutant emissions led to the improvement of air
 326 quality (increasing visibility and decreasing hazy days) in 2009 and 2010, although the
 327 atmospheric conditions remained the same and did not contributed to the spread and
 328 elimination of air pollutants. However, pollutant emissions especially in the areas of
 329 BTH rebounded after the Olympic Games, with the decrease in visibility and increase
 330 in hazy days in the BTH region around 2012 to 2014 to some extent (Zhang et al., 2015),
 331 although the atmospheric conditions remained relatively the same as before. From this
 332 result, it can be assumed the statistic estimation models for the winter mean visibility
 333 and number of hazy days would be largely influenced by an artificial control of
 334 pollutant discharge.

335



336

337 Figure 5 Curves of the observed and the predicted winter visibility (a) and number of hazy days

338

(b) in the BTH region since 1981

339

340

Table 4 List of the statistics for the Leave-N-out cross-validation estimations

N	Period covering	Visibility			Number of hazy days		
		r^2 (%)	SE	RE	r^2 (%)	SE	RE
1	1981-2015	62.7	0.74	0.61	41.5	3.37	0.38
	1981-2008	87.1	0.42	0.87	53.9	2.56	0.52
3	1981-2015	56.8	0.80	0.54	34.3	3.57	0.28
	1981-2008	86.8	0.42	0.87	52.6	2.59	0.51
5	1981-2015	59.2	0.78	0.57	35.3	3.54	0.30

	1981-2008	86.8	0.42	0.87	46.7	2.75	0.43
7	1981-2015	59.0	0.78	0.56	37.5	3.48	0.33
	1981-2008	86.4	0.43	0.86	44.7	2.80	0.41
9	1981-2015	56.2	0.80	0.54	32.5	3.62	0.27
	1981-2008	84.2	0.46	0.84	40.8	2.90	0.36
11	1981-2015	52.5	0.84	0.49	31.1	3.66	0.23
	1981-2008	84.4	0.46	0.84	48.2	2.71	0.44

(N denotes the number of sample removed in the cross-validation regressions; only the odd numbers of N were listed for short)

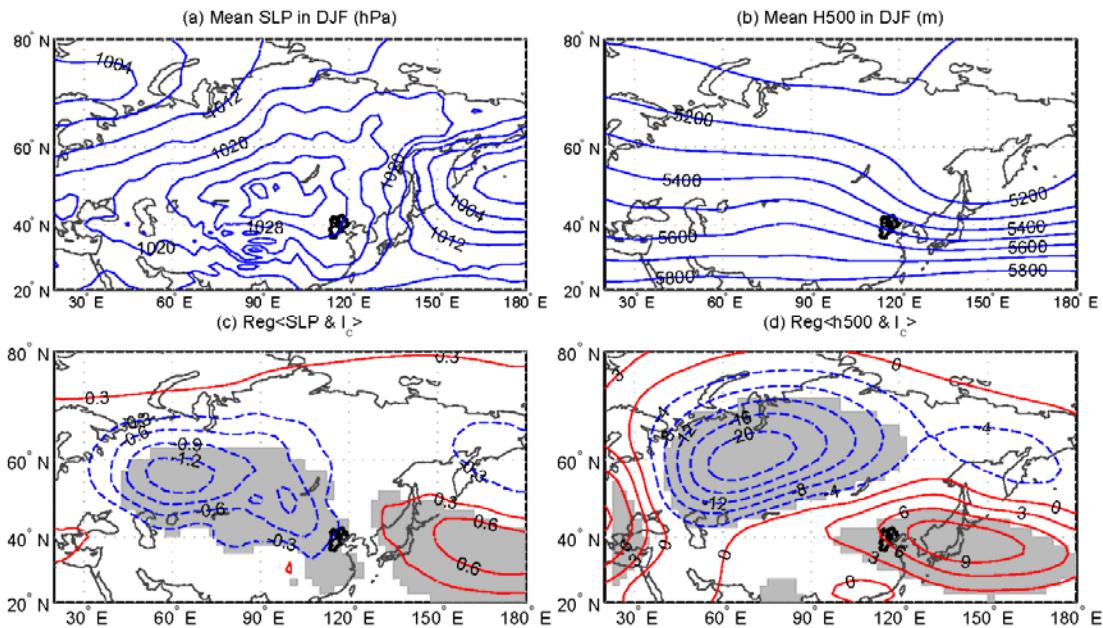
3.4 Possible mechanism of the circulations related to the winter hazy pollutions

In order to explore the possible mechanism and role of the investigated circulation indices on the winter visibility and number of hazy days in the BTH region, the links between the given large-scale atmospheric circulations and the local meteorological conditions, which have close relations with the hazy pollutions, were examined. For simplicity, a comprehensive index labeled as I_c was synthesized from the six individual circulation indices (I_1 to I_6) by applying a PCA method, namely the first principal component (PC1). The high values of the explained variance (64.4% in PC1) indicated that the comprehensive index of I_c roughly reflect the integrated features of all the six indices. Thus, we used the I_c instead of the six individual indices in the following analysis. Generally, the positive (negative) I_c indicate the lower (higher) visibility and more (less) hazy days in the BTH region in winter.

First we examined the links between the I_c and the meteorological fields of SLP and H500 respectively. Based on the NCEP/NCAR reanalysis data, Figure 6(a) and (b) present the climatological mean of SLP and H500 in winter averaged from 1981 to 2010, respectively. The changes of SLP and H500 in winter in association with a one-standard-deviation positive I_c during the winters 1981 to 2015 are shown in Figure 6(c) and (d), respectively. In the climatological mean fields, the BTH region were located in the trough of East Asian trough at the middle troposphere and in the ridge of Siberian-Mongolia high in SLP field, which indicate the northerly dominated the BTH region in winter. The regression maps show that the SLP decreased in the Siberian-Mongolia high areas and increased in the western Pacific in SLP and the geopotential height decreased in the most areas of Siberia and increased in the northern China to western Pacific. These patterns suggest that both the East Asian trough and Siberian high weaken with increasing I_c , that further implies that the winter cold air activity will be weaken and

369 then lead to an anomalous steady atmospheric conditions in BTH and its adjacent areas
 370 in winter. Namely, the less strong Siberian high and East Asian trough and associated
 371 northerly winds in the low and middle troposphere will lead to a severe hazy pollution
 372 (lower visibility and more hazy days) due to the favorable meteorological conditions
 373 for the accumulation and chemical reaction of pollutants. Anyway, we wonder whether
 374 it is true as we speculated. We further examined the links between the comprehensive
 375 index of I_c and the local meteorological conditions which play direct roles in the
 376 formation of hazy pollutions, including the wind fields (Figure 7), relative humidity
 377 (Figure 8) and vertical velocity (Figure 9) at the lowest troposphere (averaged from
 378 1000 hPa to 900 hPa with an interval of 25 hPa) and the boundary layer height (Figure
 379 10) based on the ERA-Interim reanalysis data.

380
 381



382

383 Figure 6 The climatological mean fields of SLP (a) and H500 (b) averaged in winter 1981 to 2010,
 384 and the spatial distribution of the regression coefficients of SLP (c) and H500 (d) upon the I_c over
 385 the period 1981 to 2015 (Area significant at the 0.05 level are shaded)

386

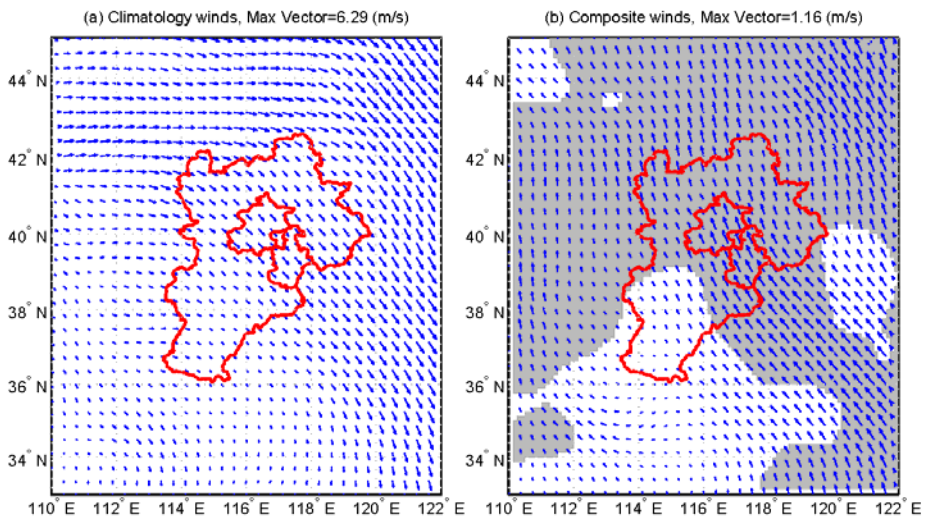
387 Figure 7(a) displays the climatological mean wind field averaged from 1000 to 900
 388 hPa over the winter 1981 to 2010. At lower level, the northwesterly winds dominated
 389 the BTH, and the wind speed in Beijing, Tianjin and north of Hebei province was larger
 390 than that in the south of Hebei province. Figure 7(b) shows the composite (positive I_c
 391 winters minus negative I_c winters) wind field averaged from 1000 to 900 hPa over the
 392 winter 1981 to 2015. In the composite wind field, the anomalous southeasterly winds

393 dominated the BTH region instead of the northwesterly in the climatological mean wind
394 field, indicating the weakening of the northwesterly significantly over BTH and its
395 neighboring areas when I_c increased. Previous studies (Zhang et al., 2015) demonstrated
396 the decreasing of wind speed is not conducive to the diffusion of air pollutants and
397 easily lead to hazy pollutions in Beijing. It may be true for the whole BTH region. Thus,
398 the increasing of I_c will lead to a decrease in the visibility and increase in the number
399 of hazy days in winter over the BTH region.

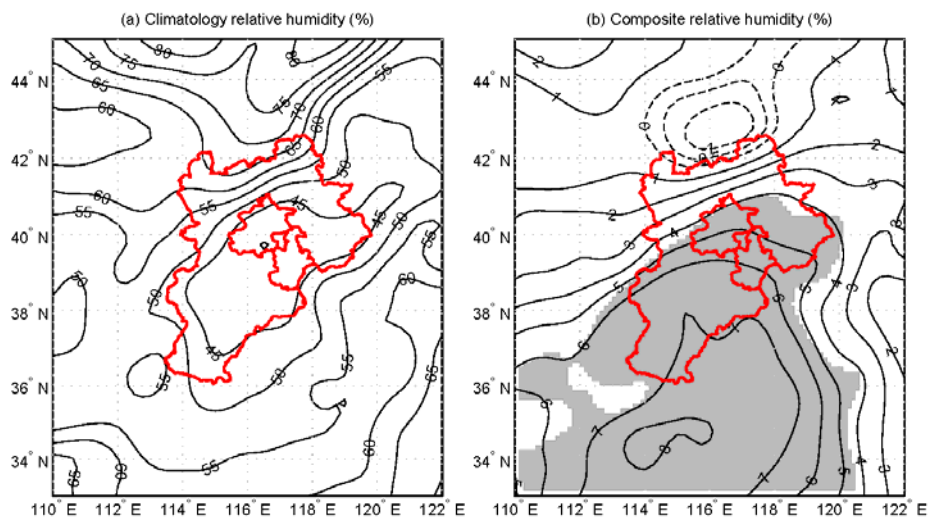
400 Same as Figure 7, Figure 8(a) and (b) present the climatology and composite
401 relative humidity averaged from the lowest troposphere respectively. In the composite
402 map, all the areas of BTH are covered by the positive values and most of them are
403 significant at the 0.05 level. They indicate that the winter relative humidity was
404 anomalous higher in the positive I_c years than that in the negative I_c years. As pointed
405 in the Introduction, a high relative humidity is one of the important reasons for visibility
406 degradation. This is because that the high relative humidity is favorable for the accumulation and
407 hygroscopic growth of pollutants, which can strengthen the light scattering and absorption by
408 atmospheric particles and gases and then cause the visibility degradation directly (Baumer et al.,
409 2008; Zhang et al., 2015). Thus a positive I_c imply that a decreasing of visibility
410 accompanied by the increasing number of hazy days may occur in the winter over BTH
411 region. Figure 9(a) and (b) present the climatology and composite vertical speeds
412 averaged from the lowest troposphere respectively. The positive (negative) values of
413 vertical speed in unit of Pa/s denote sinking (ascending) motion. The climatological
414 vertical speeds show that the downward air motions dominated the BTH region in the
415 winter. In the composite vertical speed field, the most areas of BTH were covered by
416 the significantly negative values, which suggested a less vertical exchanges of air
417 occurred in this areas in the positive I_c winters. In other words, the increased I_c may
418 result in a weaker vertical convection and forcing the lowest troposphere more stable.
419 It's easy to understand the anomalous stabilization will lead to much hazy pollutions.
420 Moreover, a similar result can be found in the planetary boundary layer height, which
421 was reduced significantly in the most of BTH and its adjacent areas in the positive I_c
422 winters (Figure 10). The decreased boundary layer height will depress the air pollutants
423 into a narrower air column in a certain area and then lead to an increasing of the
424 pollutants concentration. Thus, a winter with the lower visibility and more hazy days in
425 the BTH region would be expected in the case of the lower boundary layer height
426 caused by the anomalously high I_c .

427 In view of the responses of the local surface winds, relative humidity, vertical

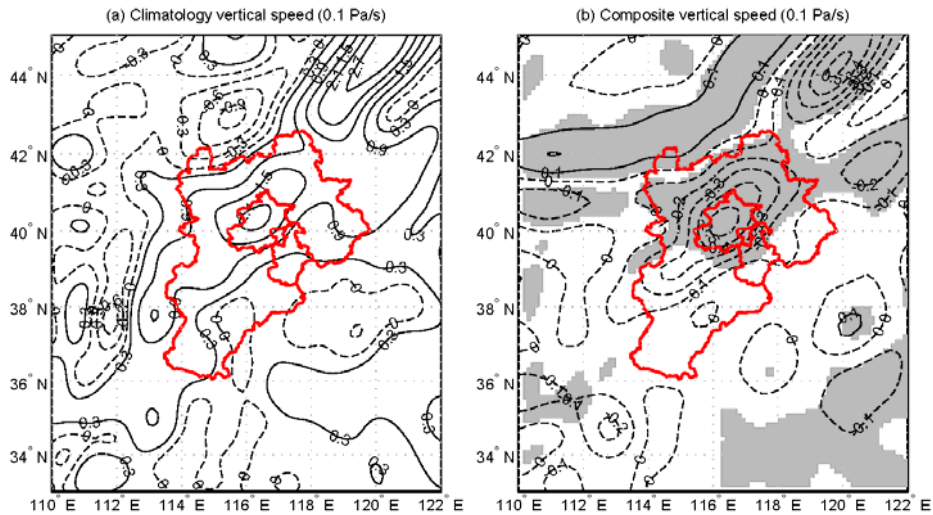
428 motion and boundary layer to the comprehensive index of I_c mentioned above, the close
 429 relationships between the winter mean visibility and number of hazy days over BTH
 430 region and the given six atmospheric circulations are generally feasible in the physical
 431 mechanism. It is reasonable and reliable to estimate the winter hazy pollutions in the
 432 BTH region based on the seasonal forecast fields derived from climate simulation. Thus
 433 it will be helpful to provide scientific references for the governmental decisions in
 434 advance about the reducing or controlling of pollutants emission to deal with the
 435 probably severe hazy pollutions in the BTH region.
 436



437
 438 Figure 7 The climatological mean (a) and the composite (b) wind fields averaged from 1000 to 900
 439 hPa (Area significant at the 0.05 level are shaded)
 440



441
 442 Figure 8 Same as Figure 7, but for relative humidity
 443

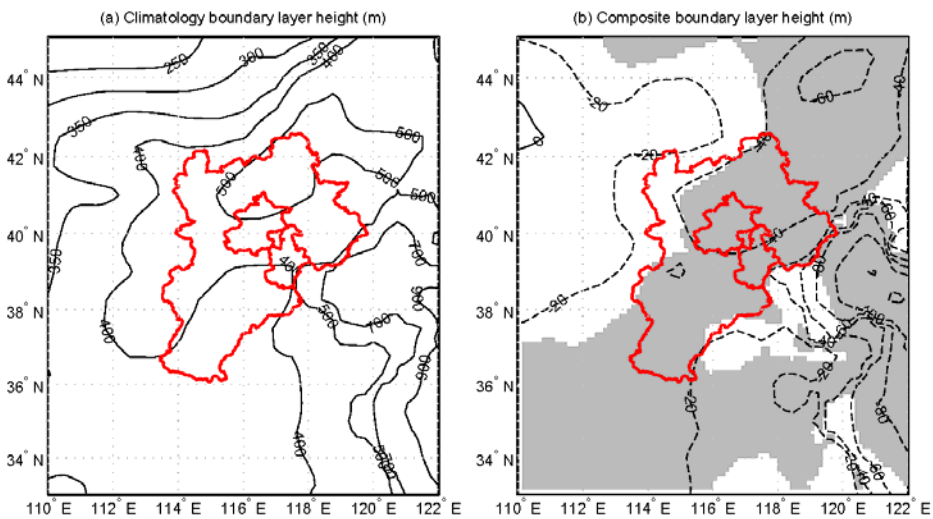


444

445

Figure 9 Same as Figure 7, but for vertical speed

446



447

448

Figure 10 The climatological mean (a) and the composite (b) boundary layer height

449

(Area significant at the 0.05 level are shaded)

450

451 4 Conclusions

452

Using the daily visibility and number of hazy days recorded in the 19
 453 meteorological stations and the NCEP/NCAR and ERA-Interim reanalysis data, the
 454 evolution of the winter hazy pollutions in the BTH region since 1981 and their possible
 455 relations to atmospheric circulations were examined in this study.

456

457

The results showed that the winter mean visibility has a significantly negative
 458 correlation with the number of hazy days and both of them show distinctly inter-annual
 459 variability during the entire period 1981 to 2015. The correlation coefficients between
 the winter hazy pollutions (the visibility and number of hazy days) and the most

460 common atmospheric circulations over the mid-high latitude of northern hemisphere
461 were re-examined. Results showed that the relations between the hazy pollutions in
462 BTH and the winter AO, NAO and PNA were very weak, but they correlated
463 significantly with EU, WP and SBH. Furthermore, the six new indices (I_1 to I_6) derived
464 from the key areas in the fields of SLP, U&V850, H500, U200 and T200 were closely
465 related to the winter hazy pollutions in BTH. We can estimate the visibility and number
466 of hazy days by using the six indices and the fitting and the leave-N-out cross-validation
467 methods, respectively. In general, the high level of the estimation statistics suggested
468 the winter hazy pollutions in BTH can be estimated or predicted in a reasonable degree
469 based on the optimized atmospheric circulation indices. However, we also noted that
470 the statistic estimation models for the visibility and number of hazy days may be
471 influenced by a prominent change of the pollutants emission artificially. Thus, it is
472 valuable and significant for government decision-making departments to take actions
473 in advance in dealing with the probably severe hazy pollutions in BTH indicated by the
474 circulation conditions, such as to control the pollutants discharge.

475 In order to investigate the link processes between the hazy pollutions and the given
476 atmospheric circulations more simply, a comprehensive index (I_c) was synthesized from
477 the six individual circulation indices by applying a PCA method. The winter I_c increase
478 appear to cause a shallowing of the East Asian trough at the middle troposphere and a
479 weakening of the Siberian high pressure field at sea level, and then accompanied by a
480 reduction (increase) of horizontal advection and vertical convection (relative humidity)
481 in the lowest troposphere and a reduced boundary layer height in BTH and its
482 neighboring areas, which are not conducive to the spread and elimination of air
483 pollutants but favor the formation of hazy pollutions in BTH winter. In short, the
484 reasonable link processes and the stable statistic relationships suggested that the
485 atmospheric circulation indices can be used to predict or evaluate generally the hazy
486 pollutions in BTH winter to some extent.

487

488 **Acknowledgments**

489 This study was supported by Beijing Natural Science Foundation (Grant no. 8152019), the National
490 Key Technologies R & D Program of China (Grant no. 2014BAC23B01 and 2014BAC23B00) and
491 Project PE15010 of the Korea Polar Research Institute. X. Zhang acknowledges the financial
492 support from the Project Z141100001014013 of Beijing Municipal Science & Technology
493 Commission. D. Gong was supported by the National Natural Science Foundation of China (Grant
494 No. 41321001).

495 **Reference:**

- 496 An, X., Zhu, T., Wang, Z., et al.: A modeling analysis of a heavy air pollution episode
497 occurred in Beijing, *Atmos. Chem. Phys.* 7, 3103–3114, 2007.
- 498 Baddock, M. C., Strong, C. L., Leys, J. F., Heidenreich, S. K., Tews, E. K., McTainsh,
499 G. H.: A visibility and total suspended dust relationship, *Atmos. Environ.*, 89, 329–
500 336, 2014.
- 501 Baumer, D., Vogel, B., Versick, S., Rinke, R., Mohler, O., Schnaiter, M.: Relationship
502 of visibility, aerosol optical thickness and aerosol size distribution in an ageing air
503 mass over South-West Germany, *Atmos. Environ.*, 42, 989–998, 2008.
- 504 Chan, C. K., Yao, X.: Air pollution in mega cities in China, *Atmos. Environ.*, 42, 1–42,
505 2008.
- 506 Chang, D., Song, Y., Liu, B.: Visibility trends in six megacities in China 1973–2007,
507 *Atmos. Res.*, 94, 161–167, 2009.
- 508 Chen, Y., Zhao, C. S., Zhang, Q., Deng, Z. Z., Huang, M. Y., Ma, X. C.: Aircraft study
509 of mountain chimney effect of Beijing, China. *J. Geophys. Res.* 114 (D8), D08306.
510 doi:10.1029/2008JD010610, 2009.
- 511 Dee, D. P., Uppala, S. M., Simmons, A. J., Berrisford, P., Poli, P., Kobayashi, S.,
512 Andrae, U., Balmaseda, M. A., Balsamo, G., Bauer, P., Bechtold, P., Beljaars, A. C.
513 M., Berg, L., Bidlot, J., Bormann, N., Delsol, C., Dragani, R., Fuentes, M., Geer, A.
514 J., Haimberger, L., Healy, S. B., Hersbach, H., Hólm, E. V., Isaksen, L., Kållberg, P.,
515 Köhler, M., Matricardi, M., McNally, A. P., Monge-Sanz, B. M., Morcrette, J. J.,
516 Park, B. K., Peubey, C., Rosnay, P., Tavolato, C., Thépaut, J. N., Vitart, F.: The ERA-
517 Interim reanalysis: Configuration and performance of the data assimilation system,
518 *Q. J. R. Meteorol. Soc.*, 137, 553–597, 2011.
- 519 Deng, J. J., Xing, Z. Y., Zhuang, B. L., Du, K.: Comparative study on long-term
520 visibility trend and its affecting factors on both sides of the Taiwan Strait, *Atmos.*
521 *Res.*, 143, 266–278, 2014.
- 522 Ding, Y. H.: A statistical study of winter monsoons in East Asia, *J. Trop. Meteor.*, 6(2),
523 119–128, 1990 (in Chinese).
- 524 Feng, J. L., Hu, M., Chan, C. K., Lau, P. S., Fang, M., He, L. Y., Tang, X. Y.: A
525 comparative study of the organic matter in PM_{2.5} from three Chinese megacities in
526 three different climatic zones, *Atmos. Environ.* 40, 3983–3994, 2006.
- 527 Fritts, H. C.: *Tree-Rings and Climate*, Academic Press, London, 567pp, 1976.
- 528 Gao, Y., Liu, X., Zhao, C., et al.: Emission controls versus meteorological conditions
529 in determining aerosol concentrations in Beijing during the 2008 Olympic Games,

530 Atmos. Chem. Phys. 11, 12437–12451, 2011.

531 Gong, D. Y., Ho, C.H.: Siberian High and climate change over middle to high latitude
532 Asia, *Theor. Appl. Climatol.*, 72, 1–9, 2002.

533 Gong, D. Y., Luterbacher, J.: Variability of the low-level cross-equatorial jet of the
534 western Indian Ocean since 1660 as derived from coral proxies. *Geophys. Res. Lett.*,
535 35, L01705, doi:1029/2007GL032409, 2008.

536 Gong, D. Y., Zhu, J. H., Wang, S. H.: The influence of Siberian High on large-scale
537 climate over continental Asia, *Plateau Meteor.*, 21(1), 8–14, 2002 (in Chinese).

538 Kalnay, E., Kanamitsu, M., Kistler, R., Collins, W., Deaven, D., Gandin, L., Iredell, M.,
539 Saha, S., White, G., Woollen, J., Zhu, Y., Leetmaa, A., Reynolds, B., Chelliah, M.,
540 Ebisuzaki, W., Higgins, W., Janowiak, J., Mo, K. C., Ropelewski, C., Wang, J., Jenne,
541 R., Joseph, D.: The NCEP/NCAR 40-year reanalysis project, *Bull. Amer. Meteor.*
542 *Soc.*, 77, 437–471, 1996.

543 Kang, H. Q., Zhu, B., Su, J. F., Wang, H. L., Zhang, Q. C., Wang, F.: Analysis of a long-
544 lasting haze episode in Nanjing, China, *Atmos. Res.*, 120, 78–87, 2013.

545 Li, Y., Lu, R. Y., He, J. H.: Several climate factors influencing the winter temperature
546 over China, *Chinese J. Atmos. Sci.*, 31(3), 505–514, 2007 (in Chinese).

547 Liu, S. H., Liu, Z. X., Li, J., Wang, Y. C., Ma, Y. J., Sheng, L., Liu, H.P., Liang, F. M.,
548 Xin, G. J., Wang, J. H.: Numerical simulation for the coupling effect of local
549 atmospheric circulations over the area of Beijing, Tianjin and Hebei Province, *Sci.*
550 *China Ser. D-Earth*, 52 (3), 382–392, 2009.

551 Lo, J. C. F., Lau, A. K. H., Fung, J. C. H., Chen, F.: Investigation of enhanced cross-
552 city transport and trapping of air pollutants by coastal and urban land-sea breeze
553 circulations. *J. Geophys. Res.* 111 (D14), D14104. doi: 10.1029/2005JD006837,
554 2006.

555 Miao, Y. C., Liu, S. H., Zheng, Y. J., Wang, S., Chen, B. C., Zheng, H., Zhao, J. C.:
556 Numerical study of the effects of local atmospheric circulations on a pollution event
557 over Beijing–Tianjin–Hebei, China, *J. Environ. Sci.*, 30, 9–20, 2015.

558 Sabetghadam, S., Farhang, A. G., Golestani, Y.: Visibility trends in Tehran during
559 1958–2008, *Atmos. Environ.* 62, 512–520, 2012.

560 Schichtel, B. A., Husar, R. B., Falke, S. R., Wilson, W. E.: Haze trends over the United
561 States 1980–1995, *Atmos. Environ.*, 35(30), 5205–5210, 2001.

562 Streets, D. G., Fu, J. H. S., Jang, C. J., Hao, J., He, K. B., Tang, X. Y., Zhang, Y. H.,
563 Wang, Z. F., Li, Z. P., Zhang, Q., Wang, L. T., Wang, B. Y., Yu, C.: Air quality
564 during the 2008 Beijing Olympic Games, *Atmos. Environ.*, 41(3), 480–492, 2007.

565 Thompson, D. W., Wallace, J. M.: The arctic oscillation signatures in the wintertime

566 geopotential height and temperature fields, *Geophys. Res. Lett.*, 25(9), 1297–1300,
567 1998.

568 Wallace, J. M., Gutzler, D. S.: Teleconnections in the geopotential height field during
569 the Northern Hemisphere winter, *Mon. Wea. Rev.*, 109, 784–812, 1981.

570 Wang, H. J., Chen, H. P., Liu, J. P.: Arctic Sea Ice Decline Intensified Haze Pollution
571 in Eastern China, *Atmos. Oceanic Sci. Lett.*, 8(1), 1–9, 2015.

572 Wang, T., Nie, W., Gao, J., Xue, L. K., Gao, X. M., Wang, X. F., Qiu, J., Poon, C. N.,
573 Meinardi, S., Blake, D., Wang, S. L., Ding, A. J., Chai, F. H., Zhang, Q. Z., and
574 Wang, W. X.: Air quality during the 2008 Beijing Olympics: secondary pollutants
575 and regional impact, *Atmos. Chem. Phys.*, 10, 7603–7615, 2010.

576 Wang, Y., Hao, J., McElroy, M. B., Munger, J. W., Ma, H., Chen, D., and Nielsen, C.
577 P.: Ozone air quality during the 2008 Beijing Olympics: effectiveness of emission
578 restrictions, *Atmos. Chem. Phys.*, 9, 5237–5251, 2009.

579 Wang, Y. S., Yao, L., Liu, Z. R., Ji, D. S., Wang, L. L., Zhang, J. K.: Formation of haze
580 pollution in Beijing-Tianjin-Hebei region and their control strategies, *Chin. Sci. Bull.*,
581 28 (3), 353–363, 2013 (in Chinese).

582 Wen, C. C., Yeh, H. H.: Comparative influences of airborne pollutants and
583 meteorological parameters on atmospheric visibility and turbidity, *Atmos. Res.*,
584 96(4), 496–509, 2010.

585 Wu, D., Chen, H. Z., Wu, M., Liao, B. T., Wang, Y. C., Liao, X. N., Zhang, X. L.,
586 Quan, J. N., Liu, W. D., Gu, Y., Zhao, X. J., Meng, J. P., Sun, D.: Comparison of
587 three statistical methods on calculating hazy days-taking areas around the capital for
588 example, *China Environ. Sci.*, 34(3), 545–554, 2014 (in Chinese).

589 Xu, W. Z., Chen, H., Li, D. H., Zhao, F. S., Yang, Y.: A case study of aerosol
590 characteristics during a haze episode over Beijing, *Procedia. Environ. Sci.* 18, 404–
591 411, 2013.

592 Zhang, Q. H., Zhang, J. P., Xue, H. W.: The challenge of improving visibility in Beijing,
593 *Atmos. Chem. Phys.* 10, 7821–7827, 2010.

594 Zhang, Q., Quan, J. L., Tie, X. X., Li, X., Liu, Q, Gao, Y., Zhao, D. L.: Effects of
595 meteorology and secondary particle formation on visibility during heavy haze events
596 in Beijing, China, *Sci. Total Environ.*, 502, 578–584, 2015.

597 Zhang, X. L., Huang, Y. B., Zhu, W. Y., Rao, R. Z.: Aerosol characteristics during
598 summer haze episodes from different source regions over the coast city of North
599 China Plain, *J. Quant. Spectrosc. Radiat. Transf.* 122, 180–193, 2013.

600 Zhang, Z. Y., Gong, D. Y., He, X. Z., Lei, Y. N., and Feng, S. H.: Statistical reconstruction of

601 Antarctic Oscillation index based on multi-proxies, *Atmos. Oceanic Sci. Lett.*, 3(5),
602 283–287, 2010.

603 Zhang, Z. Y., Gong, D. Y., Hu, M., Guo, D., He., X. Z., and Lei, Y. N.: Anomalous winter
604 temperature and precipitation events in southern China, *J. Geogra. Sci.*, 19(4), 471–
605 488, 2009.

606 Zhang, Z. Y., Zhang, X. L., Gong, D. Y., Quan, W. J., Zhao, X. J., Ma, Z. Q., and Kim, S. J.: Evolution
607 of surface O₃ and PM_{2.5} concentrations and their relationships with meteorological
608 conditions over the last decade in Beijing, *Atmos. Environ.*, 108, 67–75, 2015.

609 Zhao, X. J., Zhang, X. L., Xu, X. F., Xu, J., Meng, W., and Pu, W. W.: Seasonal and diurnal
610 variations of ambient PM_{2.5} concentration in urban and rural environments in Beijing,
611 *Atmos. Environ.* 43, 2893–2900, 2009.

612 Zhao, X. J., Zhao, P. S., Xu, J., Meng, W., Pu, W. W., Dong, F., He, D., and Shi, Q. F.: Analysis of a
613 winter regional haze event and its formation mechanism in the North China Plain,
614 *Atmos. Chem. Phys.*, 13, 5685–5696, 2013.

615

616